



Published in final edited form as:

Arthritis Rheum. 2012 November ; 64(11): 3695–3705. doi:10.1002/art.34642.

Two Independent Functional Risk Haplotypes in *TNIP1* are Associated with Systemic Lupus Erythematosus

Indra Adrianto^{1,*}, Shaofeng Wang^{1,*}, Graham B. Wiley^{1,*}, Christopher J. Lessard^{1,2}, Jennifer A. Kelly¹, Adam J. Adler¹, Stuart B. Glenn¹, Adrienne H. Williams³, Julie T. Ziegler³, Mary E. Comeau³, Miranda C. Marion³, Benjamin E. Wakeland⁴, Chaoying Liang⁴, Kenneth M. Kaufman^{5,6}, Joel M. Guthridge¹, Marta E. Alarcón-Riquelme^{1,7}, on behalf of the BIOLUPUS and GENLES Networks, Graciela S. Alarcón⁸, Juan-Manuel Anaya⁹, Sang-Cheol Bae¹⁰, Jae-Hoon Kim¹⁰, Young Bin Joo¹⁰, Susan A. Boackle¹¹, Elizabeth E. Brown¹², Michelle A. Petri¹³, Rosalind Ramsey-Goldman¹⁴, John D. Reveille¹⁵, Luis M. Vilá¹⁶, Lindsey A. Criswell¹⁷, Jeffrey C. Edberg⁸, Barry I. Freedman¹⁸, Gary S. Gilkeson¹⁹, Chaim O. Jacob²⁰, Judith A. James^{1,2}, Diane L. Kamen¹⁹, Robert P. Kimberly⁸, Javier Martin²¹, Joan T. Merrill²², Timothy B. Niewold²³, Bernardo A. Pons-Estel²⁴, R. Hal Scofield^{1,2,25}, Anne M. Stevens^{26,27}, Betty P. Tsao²⁸, Timothy J. Vyse²⁹, Carl D. Langefeld³, John B. Harley^{5,6}, Edward K. Wakeland⁴, Kathy L. Moser^{1,2}, Courtney G. Montgomery^{1,**}, and Patrick M. Gaffney^{1,**}

¹Arthritis and Clinical Immunology Research Program, Oklahoma Medical Research Foundation, Oklahoma City, OK

²College of Medicine, University of Oklahoma Health Sciences Center, Oklahoma City, OK

Corresponding Author: Patrick M. Gaffney, M.D., Arthritis and Clinical Immunology Research Program, Oklahoma Medical Research Foundation, 825 N.E. 13th Street, MS #57, Oklahoma City, OK 73104, Phone: 405-271-2572, Fax: 405-271-2536, gaffneyp@omrf.org.

*These authors contributed equally to this work.

**These authors jointly directed this work.

The authors declare no competing financial interests.

Web Resources

The URLs for data presented herein are as follows:

Online Mendelian Inheritance in Man (OMIM), <http://www.ncbi.nlm.nih.gov/Omim/PolyPhen-2> (Polymorphism Phenotyping v2), <http://genetics.bwh.harvard.edu/pph2/>

Author Contributions

Substantial contributions to study conception and design

Indra Adrianto, Shaofeng Wang, Graham B. Wiley, Christopher J. Lessard, Adrienne H. Williams, Miranda C. Marion, Benjamin E. Wakeland, Chaoying Liang, Kenneth M. Kaufman, Joel M. Guthridge, Marta E. Alarcón-Riquelme, Rosalind Ramsey-Goldman, Jeffrey C. Edberg, Barry I. Freedman, Chaim O. Jacob, Javier Martin, Carl D. Langefeld, John B. Harley, Edward K. Wakeland, Kathy L. Moser, Courtney G. Montgomery, Patrick M. Gaffney

Substantial contributions to acquisition of data

Indra Adrianto, Shaofeng Wang, Graham B. Wiley, Christopher J. Lessard, Jennifer A. Kelly, Adam J. Adler, Stuart B. Glenn, Benjamin E. Wakeland, Chaoying Liang, Kenneth M. Kaufman, Joel M. Guthridge, Marta E. Alarcón-Riquelme, Graciela S. Alarcón, Juan-Manuel Anaya, Sang-Cheol Bae, Jae-Hoon Kim, Young Bin Joo, Susan A. Boackle, Elizabeth E. Brown, Michelle A. Petri, Rosalind Ramsey-Goldman, John D. Reveille, Luis M. Vila, Lindsey A. Criswell, Jeffrey C. Edberg, Barry I. Freedman, Gary S. Gilkeson, Chaim O. Jacob, Judith A. James, Diane L. Kamen, Robert P. Kimberly, Javier Martin, Joan T. Merrill, Timothy B. Niewold, Bernardo A. Pons-Estel, R. Hal Scofield, Anne M. Stevens, Betty P. Tsao, Timothy J. Vyse, Carl D. Langefeld, John B. Harley, Edward K. Wakeland, Kathy L. Moser, Courtney G. Montgomery, Patrick M. Gaffney

Substantial contributions to analysis and interpretation of data

Indra Adrianto, Shaofeng Wang, Graham B. Wiley, Christopher J. Lessard, Adrienne H. Williams, Julie T. Ziegler, Mary E. Comeau, Miranda C. Marion, Kenneth M. Kaufman, Elizabeth E. Brown, Javier Martin, Carl D. Langefeld, Kathy L. Moser, Courtney G. Montgomery, Patrick M. Gaffney

Drafting the article or revising it critically for important intellectual content

All authors

Final approval of the version of the article to be published

All authors

- ³Department of Biostatistical Sciences, Wake Forest School of Medicine, Winston-Salem, NC
- ⁴Department of Immunology, University of Texas Southwestern Medical Center, Dallas, TX
- ⁵Division of Rheumatology, Cincinnati Children's Hospital Medical Center, Cincinnati, OH
- ⁶US Department of Veterans Affairs Medical Center, Cincinnati, OH
- ⁷Centro de Genómica e Investigaciones Oncológicas (GENyO), Pfizer-Universidad de Granada-Junta de Andalucía Granada, Spain
- ⁸Department of Medicine, University of Alabama at Birmingham, Birmingham, AL
- ⁹Center for Autoimmune Diseases Research (CREA), Universidad del Rosario, Bogotá, Colombia
- ¹⁰Department of Rheumatology, Hanyang University Hospital for Rheumatic Diseases, Seoul, Republic of Korea
- ¹¹Division of Rheumatology, University of Colorado Denver, Aurora, CO
- ¹²Department of Epidemiology, University of Alabama at Birmingham, Birmingham, AL
- ¹³Department of Medicine, Johns Hopkins University School of Medicine, Baltimore, MD
- ¹⁴Division of Rheumatology, Northwestern University Feinberg School of Medicine, Chicago, IL
- ¹⁵Rheumatology and Clinical Immunogenetics, University of Texas Health Science Center at Houston, Houston, TX
- ¹⁶Department of Medicine, Division of Rheumatology, University of Puerto Rico Medical Sciences Campus, San Juan, Puerto Rico
- ¹⁷Rosalind Russell Medical Research Center for Arthritis, University of California San Francisco, San Francisco, CA
- ¹⁸Department of Internal Medicine/Nephrology, Wake Forest School of Medicine, Winston-Salem, NC
- ¹⁹Division of Rheumatology, Medical University of South Carolina, Charleston, SC
- ²⁰Department of Medicine, University of Southern California, Los Angeles, CA
- ²¹Instituto de Parasitología y Biomedicina "López-Neyra", Consejo Superior de Investigaciones Científicas (CSIC), Granada, Spain
- ²²Clinical Pharmacology Research Program, Oklahoma Medical Research Foundation, Oklahoma City, OK
- ²³Section of Rheumatology and Gwen Knapp Center for Lupus and Immunology Research, University of Chicago, Chicago, IL
- ²⁴Sanatorio Parque, Rosario, Argentina
- ²⁵US Department of Veterans Affairs Medical Center (DVAMC), Oklahoma City, OK
- ²⁶Division of Rheumatology, Department of Pediatrics, University of Washington, Seattle, WA
- ²⁷Center for Immunity and Immunotherapies, Seattle Children's Research Institute, Seattle, WA
- ²⁸Division of Rheumatology, Department of Medicine, University of California Los Angeles, Los Angeles, CA
- ²⁹Divisions of Genetics and Molecular Medicine and Immunology, Infection and Inflammatory Diseases, King's College London, London, UK

Abstract

Objective—Systemic lupus erythematosus (SLE) is an autoimmune disease characterized by autoantibody production and altered type I interferon expression. Genetic surveys and genome-wide association studies have identified more than 30 SLE susceptibility genes. One of these genes, *TNIP1*, encodes the ABIN1 protein. ABIN1 functions in the immune system by restricting the NF- κ B signaling. In order to better understand the genetic factors that influence association with SLE in genes that regulate the NF- κ B pathway, we analyzed a dense set of genetic markers spanning *TNIP1* and *TAX1BP1*, as well as the *TNIP1* homolog, *TNIP2*, in case-control sets of diverse ethnic origins.

Methods—We fine-mapped *TNIP1*, *TNIP2*, and *TAX1BP1* in a total of 8372 SLE cases and 7492 healthy controls from European-ancestry, African-American, Hispanic, East Asian, and African-American Gullah populations. Levels of *TNIP1* mRNA and ABIN1 protein were analyzed using quantitative RT-PCR and Western blotting, respectively, in EBV-transformed human B cell lines.

Results—We found significant associations between genetic variants within *TNIP1* and SLE but not in *TNIP2* or *TAX1BP1*. After resequencing and imputation, we identified two independent risk haplotypes within *TNIP1* in individuals of European-ancestry that were also present in African-American and Hispanic populations. These risk haplotypes produced lower levels of *TNIP1* mRNA and ABIN1 protein suggesting they harbor hypomorphic functional variants that influence susceptibility to SLE by restricting ABIN1 expression.

Conclusion—Our results confirmed the association signals between SLE and *TNIP1* variants in multiple populations and provide new insight into the mechanism by which *TNIP1* variants may contribute to SLE pathogenesis.

Introduction

The Nuclear factor kappa B (NF- κ B) family of transcription factors are key mediators of innate and adaptive immune responses. A diverse array of surface receptors including Tumor Necrosis Factor-alpha (TNF α) and Toll-like receptors (TLRs) converge on NF- κ B (1, 2), therefore, precise control of NF- κ B is required to effectively interpret and transmit these signals in order to produce an effective defense against invading pathogens and viruses. The ubiquitin editing enzyme, A20, encoded by tumor necrosis factor-alpha inducible protein 3 (*TNFAIP3*, OMIM 191163), is a critical negative regulator of NF- κ B (3, 4). Termination of NF- κ B signaling by A20 leverages adapter proteins such as Tax1 (human T-cell leukemia virus type I) binding protein 1 (*TAX1BP1*, OMIM 605326) and the A20 binding inhibitor of NF- κ B1 (ABIN1), which facilitate the interaction of A20 with target molecules (5, 6). Breakdown of this system leads to unrestrained NF- κ B transactivation that can result in autoimmune diseases, sepsis, and/or malignancy (7–10).

Systemic lupus erythematosus (SLE, OMIM 152700) is an autoimmune disease that demonstrates a robust but complex genetic architecture. Candidate gene and genome-wide association studies have identified over 30 genetic loci convincingly associated with SLE (11–13). Among these are *TNFAIP3* and *TNFAIP3* interacting protein 1 (*TNIP1*, OMIM 607714), which encodes ABIN1, emphasizing the importance of these genes in restricting autoimmunity. Variants in the vicinity of *TNFAIP3* are associated with multiple autoimmune diseases in multiple ethnic populations (14–16). Moreover, multiple independent genetic effects associated with SLE appear to be operating in the region (17–19). Our group recently identified a functional polymorphism in a regulatory element ~25 kb telomeric of the *TNFAIP3* coding region that can explain the association signal of one of these independent effects (20).

Variants in the region of *TNIP1* are also associated with multiple autoimmune diseases, including psoriasis (21) (OMIM 177900), psoriatic arthritis (22) (OMIM 607507), systemic sclerosis (23) (OMIM 181750), and SLE (24, 25). However, in contrast to *TNFAIP3*, less is known about the genetic architecture of *TNIP1*. For instance, association with *TNIP1* has only been evaluated in SLE cases of European and Asian ancestry (24, 25), thus it is not known if *TNIP1* is a risk locus in African American and Hispanic populations. Furthermore, *TNIP1* has not been thoroughly fine-mapped to determine the number of risk effects present in the region, nor have any functional mechanisms have been attributed to *TNIP1* associated risk haplotypes.

In order to gain a more comprehensive understanding of the *TNIP1* locus in SLE we performed a genetic fine-mapping study in five ethnically diverse SLE case-control collections. We also included single-nucleotide polymorphisms (SNPs) in *TAX1BP1*, an adapter molecule for A20 (5) located adjacent to the previously described SLE susceptibility gene JAZF zinc finger 1 (*JAZF1*, OMIM606246) and in the *TNIP1* homolog, *TNFAIP3* interacting protein 2 (*TNIP2*, OMIM 610669). Our results demonstrate a complex genetic architecture within the *TNIP1* locus that is shared, in part, across multiple ethnic populations. We identify two independent functional risk haplotypes that result in decreased expression of *TNIP1* mRNA and ABIN1 protein, providing insight into the mechanism by which variants in *TNIP1* may contribute to SLE pathogenesis.

Patients and Methods

Subjects

The following groups of independent cases and controls were included in the study (Supplementary Table 1): European-ancestry (EA, 4,248 cases and 3,818 controls), African-American (AA, 1,569 cases and 1,893 controls), Hispanic enriched for the Amerindian-European admixture (HS, 1,622 cases and 887 controls), East Asian (AS, 1,328 cases and 1,348 controls), and African-American Gullah (AAG, 155 cases and 131 controls) populations. The majority of AS samples were from Korea (906 cases and 1012 controls) but also included Chinese, Japanese, Taiwanese and Singaporeans. The AAG population is a group of African Americans originating from Sierra Leone with low genetic admixture who live in the Sea Islands of the Carolinas. All cases met the 1997 ACR revised criteria for the classification of SLE (26). Samples were supplied from multiple institutions with the approval from their respective Institutional Review Boards (IRBs); consent forms were obtained at each place under IRB guidelines. Samples were then assembled at the Oklahoma Medical Research Foundation (OMRF) under the approval of the OMRF IRB. Only individuals who signed informed consent forms were included in the study.

Genotyping and Quality Control

Genotyping was performed on the Illumina iSelect platform at OMRF for 88, 22, and 52 SNPs within and flanking *TNIP1* on chromosome 5q33, *TAX1BP1* on chromosome 7p15, and *TNIP2* on chromosome 4p16, respectively, as well as 347 genome-wide ancestry-informative markers (AIMs) (27, 28) (Supplementary Table 2). For inclusion we required SNPs to have well-defined cluster scatter plots, a call rate >90%, a minor allele frequency >0.001 and Hardy-Weinberg proportion test *P*-value in controls >0.001. For the AIMs, we excluded AIMs with low call rates (<90%), low minor allele frequencies (<0.001), and that are in LD with each other ($r^2 > 0.2$). The Hardy-Weinberg proportion test was not performed here to avoid AIMs being removed due to monomorphic states in one of the populations. A total of 1,135 samples were excluded because they were sample heterozygosity outliers (>5 standard deviations from the mean), extreme population outliers (based on global ancestry estimation and principal component analysis), sample duplicates (the proportion of alleles

shared identity by descent >0.4), had a low call rate ($<90\%$), or gender discrepancies between reported gender and genetic data (Supplementary Table 3). Using 262 AIMs, principal components analysis (29), calculated using R (Supplementary Figure 1), and global ancestry, estimated using ADMIXMAP (30, 31), were used to identify population outliers (>4 standard deviation from the mean of principal components 1 and 2 with ancestral allele frequencies from African, European, American Indian, and East Asian populations) and estimate percent ancestry for inclusion in association analysis as an adjustment for population substructure. After applying sample and SNP quality control measures, the final dataset was comprised of the samples and SNPs shown in Table 1 and Supplementary Table 4, respectively.

Association Analyses

Single-marker associations were assessed using the logistic regression function in PLINK v1.07 (32) and R version 2.12.0, assuming an additive model and adjusting for gender and either global ancestry (African, European, and East Asian) or the first three principal components, with no observable difference. We set a stringent Bonferroni corrected P -value threshold of $P < 3.21 \times 10^{-4}$ based on multiple tests of 156 genotyped SNPs (0.05/156). The association results were plotted using LocusZoom (33).

Resequencing, Variant Detection and Quality Control

Three to five micrograms of genomic DNA from a set of 296 European, 41 African American and 40 Hispanic individuals enriched for known SLE risk haplotypes were sheared and prepared for sequencing using the Illumina Paired-End Genomic DNA Sample Prep Kit (Illumina Inc., San Diego, CA). The region of interest enrichment was performed using a SureSelect Target Enrichment System with a custom designed bait pool. Resequencing and generation of fastq sequencing reads were performed on the Illumina GAIIx platform and Illumina Pipeline software v.1.7 using standard procedures.

We removed duplicate reads using a custom script followed by alignment to the human reference genome build hg19 using BWA alignment software version 0.5.9 (34). Realignment of reads around insertion/deletion sites and problematic areas, base quality score recalibration, and variation detection were performed using the Genome Analysis Tool Kit (GATK) software suite version 1.0 (35, 36). We excluded variants with a quality score < 30 , a quality by depth score < 5 , inclusion within a homopolymer run of 5 or more bases, or a strand bias score of > -0.1 , as well as variants clustered within 10 base pairs. All samples were sequenced to minimum average fold coverage of 25X. We compared sequence-based variant calls with SNPs previously genotyped on the Illumina iSelect platform and found $> 99\%$ concordance between platforms. The program BEAGLE version 3.3 (37) was used to determine variant phase. PLINK version 1.07 and IMPUTE2 (38) format files were generated using the vcftools software suite version 0.1.3 (39).

Imputation and Haplotype Analyses

Imputation was performed over a 500 kb interval flanking the *TNIP1* region for each population using the IMPUTE2 program with data from iSelect genotyping as the source of observed genotypes and the haplotypes from the 1000 Genomes Project Phase I interim release (June 2011) for 1,094 individuals from Africa, Asia, Europe, and the Americas (40) (Supplementary Table 5) and our in-house sequencing as reference. IMPUTE2 estimates posterior probabilities for the three possible genotypes of imputed SNPs (i.e. AA, AB, and BB). Association analyses of imputed SNPs were calculated using a missing data likelihood score test implemented in SNPTEST version 2.3.0 by taking into account the genotype uncertainty of imputed SNPs and adjusting for gender and global ancestry estimates (41). Conditional association analyses were also performed in SNPTEST adjusting for gender,

global ancestry estimates, and SNP(s) of interest within the risk haplotypes. For haplotype analyses, the posterior probabilities were converted to the most likely genotypes with a threshold of 0.8. Imputed SNPs with the information measure less than 0.5, the average maximum posterior genotype call probability less than 0.9 or failed quality control measures were removed. Linkage disequilibrium (LD) between variants (confirmed by the r^2 values) and haplotypes were estimated followed by haplotypic association using Haploview version 4.2 (42). The number of variants imputed from the 1000 Genomes Project and our sequencing data that passed quality control measures can be found in Supplementary Table 4.

Cell Culture

EBV-transformed B cell lines of EA individuals were obtained from the Lupus Family Registry and Repository (LFRR) (43) at OMRF with an IRB approval and were selected based on the genotypes of rs7719549 (a proxy of the H1 haplotype) and rs33934794 (a proxy of the H2 haplotype). Cell lines are either homozygous (carry two copies) of non-risk haplotype or homozygous (carry two copies) of each risk haplotype. Culturing of cell lines was performed in RPMI 1640 supplemented with 10% fetal bovine serum, penicillin, streptomycin, L-glutamine, and 55 μ M beta-mercaptoethanol. We harvested equal numbers of cells under basal conditions in log-phase growth.

RNA Isolation and Quantitative RT-PCR

The isolation of total RNA was performed using the Trizol total RNA isolation reagent (Invitrogen Inc., Carlsbad, CA). The concentrations of total RNA were measured using nanodrop, and were diluted with 20ng/ μ L of MS2-RNA (Hoffmann-La Roche, Inc., Nutley NJ) to a final concentration of 0.5 μ g/ μ L. Total RNA was treated with DNase and cDNA was synthesized using the iScript cDNA Synthesis Kits (Bio-Rad Laboratories, Inc., Hercules, CA). Quantitative PCR was done using the SYBR Green method to determine the mRNA expression of *TNIP1*. The following pair of primers were designed and synthesized: sense, 5'-AAATCCAAATCAGAGCTCCCAA-3'; anti-sense, 5'-CAAATGACACAATCTGGTCTCACT-3'. The PCR product corresponds to 2407bp-2519bp of *TNIP1* mRNA. We used the human hydroxymethylbilane synthase (*HMBS*) gene in quantitative RT-PCR as a reference. The RT² qPCR Primer Assay-SYBR Green Human *HMBS* Kit was obtained from SABiosciences Inc., Frederick, MD. The mRNA expression of *TNIP1* was normalized to *HMBS*. Statistical analyses were performed using an unpaired *t*-test on Prism 5.0 software.

Analysis of Protein Expression

We harvested and lysed EBV-transformed B cells in Whole Cell Extraction Buffer (25mM Tris, 1% Triton X-100, 150mM NaCl, 1mM EDTA and protease inhibitors). Protein concentrations in each cell line were measured using Quick Start Bradford Protein Assay Kits and were adjusted to a final protein concentration of 2mg/mL. Anti-ABIN1 antibodies (kindly provided by Drs. Sambit Nanda and Philip Cohen, MRC Protein Phosphorylation Unit, University of Dundee, Dundee, DD1 5EH, Scotland, UK) were used to detect ABIN1 protein expression in EBV cell lines. The generation and characterization of this antibody is described in Nanda *et al* (44). Anti-GAPDH (glyceraldehyde-3-phosphate dehydrogenase) antibodies were procured from Cell Signaling Technology, Inc. and were used to detect protein expression of GAPDH. ECL Plus Western blotting detection kit was purchased from GE Healthcare, Inc. and was used to visualize horseradish-peroxidase conjugated antibodies. Band intensities were analyzed using Image J (NIH) software. Protein expression of ABIN1 was normalized to GAPDH. The expression differences were tested using an unpaired *t*-test on Prism 5.0 software.

Results

To test for genetic association, we performed single-marker logistic regression analysis adjusting for gender and global ancestry estimated using AIMs (Patients and Methods). We found no convincing association exceeding a Bonferroni corrected threshold of $P < 3.21 \times 10^{-4}$ in *TAX1BP1* or *TNIP2* for any of the populations (Supplementary Figures 2 and 3), however, rs232722, located downstream of *TNIP2*, demonstrated suggestive association in the AS cohort ($P = 8.91 \times 10^{-4}$, OR = 0.83, 95% CI = 0.74 – 0.92) (Supplementary Figure 3D). In contrast, significant association was observed for SNPs in *TNIP1* in the EA (rs6889239; $P = 2.24 \times 10^{-11}$), AA (rs13168551; $P = 5.86 \times 10^{-5}$) and HS (rs7708392; $P = 2.02 \times 10^{-6}$) populations (Figures 1A–C). In the AS population we observed association slightly below the Bonferroni corrected threshold (rs4958435; $P = 5.49 \times 10^{-4}$, Figure 1D) while no significant association was observed in the AAG (Supplementary Figure 4). The AS population consisted of 71% Koreans and, when analyzed independently, resulted no marked differences in association from the Korean dataset; hence, subsequent analyses were performed on the full AS dataset. The presence of multiple associated SNPs with variable pairwise LD in the EA, AA and HS populations suggested that multiple independent SLE associated haplotypes are present in the region (Figure 1).

Before proceeding to evaluate *TNIP1* using haplotype and conditional analyses, we sought to enrich our genotype dataset by imputing untyped variants in linkage disequilibrium (LD) with SLE associated SNPs. To do this, we imputed variants from the 1000 Genomes Project (1TGP) using reference panels from individuals of European, African, Asian and Amerindian ancestry (Supplementary Table 4). This procedure increased the number of variants in all populations and added to the dataset 19 to 30 additional variants in LD with directly genotyped SLE associated SNPs (Supplementary Table 4). As a further enrichment step for causal variants we imputed variants from an independent resequencing study of EA SLE cases (N=159) and controls (N=137), AA cases (N=21) and controls (N=20), and HS cases (N=38) performed in our laboratory. This procedure added 13 to 30 novel variants not present in the 1TGP reference panels, five of which were in moderate to high LD (two variants with $r^2 = 0.71$ and three variants with $r^2 = 0.99$) with SLE associated genotyped SNPs (Supplementary Table 4). In total, imputation of variants from the 1TGP and our own resequencing introduced 24 to 35 (depending on the population) SLE associated variants into consideration. Association analyses using these enriched datasets demonstrated enhanced granularity of the association signals, although the most significant signals in the EA, AA, and HS populations remained constant (Figure 1). In the case of the AS, however, the peak association signals shifted approximately 6 kb centromeric from rs4958435 to rs2112635 ($P = 2.00 \times 10^{-4}$, OR = 0.74, 95% CI = 0.63 – 0.88) (Figure 1D).

To investigate the presence of multiple SLE associated haplotypes in *TNIP1*, we constructed haplotypes using SNPs that surpassed the Bonferroni corrected threshold of $P < 3.21 \times 10^{-4}$ (Table 2). In the EA population we observed two risk haplotypes, H1 and H2, spanning 29 kb of the *TNIP1* region (Figure 2). Of the 42 SNPs carried on H1 and the 19 SNPs carried on H2, 11 were found on both risk haplotypes and produced the most significant association signals (Figure 2). To determine if these haplotypes defined independent association signals, we performed conditional analyses. Conditioning on variants unique to H1 did not significantly change the magnitude of association for SNPs unique to H2, but did reduce the magnitude of the association for the SNPs shared by both risk haplotypes by about one half (Supplementary Figure 5A). Likewise, adjusting for the H2 haplotype failed to reduce the magnitude of association at variants unique to H1, while again reducing the magnitude of association for the shared SNPs (Supplementary Figure 5B). Adjusting for both H1 and H2 effectively eliminated the association signals in the region (Supplementary Figure 5C), thus confirming the presence of two independent risk haplotypes.

We then looked for these haplotypes in the other populations. H1 was present in the AA and HS populations but we did not observe it in the AS population at a haplotype frequency above 3% (Table 3, Supplementary Figure 6, Supplementary Table 6). The frequency of H1 differed across populations and was more prevalent in the AA than any other population. H2 was observed in the AA, HS, and AS populations (Table 3, Supplementary Figure 6, Supplementary Table 6). The AS population had the highest prevalence of the H2 haplotype but it was evenly distributed between cases and controls and not associated with SLE. The odds ratios for both haplotypes in the AA and HS populations ranged from 1.31 to 1.45 indicating that they also conferred risk for SLE. Conditional analyses in these populations confirmed that they were independent (Supplementary Figures 7 and 8).

To evaluate the effects of the *TNIP1* risk haplotypes on mRNA expression, quantitative RT-PCR was performed in an independent set of EA derived EBV-transformed B cell lines homozygous for H1 (N=7), H2 (N=7), and the non-risk haplotype (N=8). Compared with cells from the non-risk haplotype, cells homozygous for H1 ($P = 0.044$) or H2 ($P = 0.0035$) exhibited decreased mRNA expression of *TNIP1* (Figure 3A).

Western blotting was also performed in the same independent set of EBV-transformed B cells to evaluate the effects of the risk haplotypes on protein expression of ABIN1. Compared with cells from the non-risk haplotype and concordant with mRNA measurements, decreased ABIN1 expression was observed in cells homozygous for H1 ($P = 0.0463$) or H2 ($P = 0.0002$) (Figure 3B and Supplementary Figure 9). Together, these data suggest that both haplotypes harbor hypomorphic risk variants that influence autoimmune susceptibility by reducing expression of ABIN1.

Discussion

In this study, we genetically dissected the *TNIP1* locus in a multi-ethnic SLE case-control sample collection. Using haplotype and conditional analyses and a comprehensive variant dataset derived from direct genotyping and imputation of variants from the public domain and targeted deep resequencing, we identified two independent risk haplotypes (H1 and H2) in the EA, AA, and HS populations. These risk haplotypes likely carry hypomorphic functional alleles since cell lines derived from EA individuals with these haplotypes demonstrated reduced expression of *TNIP1* mRNA and ABIN1 protein.

In addition to our study, a study of systemic sclerosis also demonstrated decreased expression of *TNIP1* mRNA and ABIN1 protein in both lesional skin tissue and cultured dermal fibroblasts (23). They identified rs2233287, rs4958881, and rs3792783 (all within the H1 haplotype) as associated with disease (23). While the samples were not stratified by genotype, decreased expression in diseased tissue and association with what appears to be one of the risk haplotypes we have identified in SLE suggests the possibility of a shared mechanism in the etiologies of systemic sclerosis and SLE.

TNIP1 encodes the adapter protein ABIN1, which recruits A20 to polyubiquitinated NEMO (IKK γ) and subsequently facilitates NEMO deubiquitination and restriction of NF- κ B signaling (45) making it a compelling candidate for SLE susceptibility. The importance of ABIN1 in restricting NF- κ B signaling has been shown in mice deficient for ABIN1, which succumb to hepatocyte apoptosis, anemia and bone marrow hypoplasia *in utero* (46). Moreover, mice expressing a mutated ABIN1 that is defective in polyubiquitin-binding develop lupus-like autoimmunity (44). Embryonic fibroblasts from ABIN1-deficient mice or mice expressing polyubiquitin-binding defective ABIN1 also demonstrated hypersensitivity to TNF-induced apoptosis (44, 46). The ABIN1 interaction with polyubiquitin chains, including linear and K63 polyubiquitin chains, suppressed the activation of TLR-MyD88

signaling that is important to prevent autoimmune disease (44). The loss of ABIN1 has also been shown to increase the expression of TLR-induced CCAAT/enhancer binding protein β (C/EBP β) resulting in the development of a lupus-like inflammatory disease (47). The H1 haplotype also carries the minor allele of a coding missense variant rs2233290, which results in a proline to alanine substitution at position 151 in ABIN1. The P151A polymorphism is predicted to be damaging according to PolyPhen-2 version 2.1.0 (48) and represents a putative causal variant for future functional studies.

The H1 and H2 haplotypes include SNPs near the *TNIP1* promoter and it is therefore likely that causal variants located within regulatory elements affect *TNIP1* gene expression. A recent study has functionally validated five NF- κ B binding sites in the *TNIP1* promoter that potentially influence *TNIP1* expression (49). However, none of these NF- κ B binding sites are modified by SNPs carried on the SLE associated haplotypes.

We did not identify any significant association between SLE and variants in the other genes investigated: *TNIP2* and *TAX1BP1*. We did however observe modest association in the *TNIP2* region for the AS population, warranting further study in larger AS SLE sample collections. Note, that our *TAX1BP1* fine-mapping SNP panel was near, but did not overlap sufficiently with the *JAZF1* locus, known to be associated with SLE in individuals of European-ancestry (24). Thus, we cannot provide independent replication of the *JAZF1* association. However, our results are likely sufficient to rule out an effect from *TAX1BP1* being responsible for, or contributing to, the association in *JAZF1*.

In summary, our results clarify the association signals in the *TNIP1* locus in human SLE across multiple ethnic populations and suggest that reduced expression of ABIN1 contributes to SLE pathogenesis. Our data also inform ongoing efforts to identify *TNIP1* causal variants in other autoimmune diseases by clarifying the genetic architecture of the locus across multiple world populations. In addition, this trans-ethnic mapping study design has been successful in narrowing other SLE associated regions including the *ITGAM* and *TNFAIP3* loci (20, 50). Given the importance of ABIN1 in restricting NF- κ B signaling, a mechanistic understanding of how deleterious genetic variation in the *TNIP1* locus influences susceptibility to autoimmune disease is needed. These results will serve to focus functional hypotheses that can be tested in the laboratory.

Supplementary Material

Refer to Web version on PubMed Central for supplementary material.

Acknowledgments

Funding Information

Support for this work was obtained from the US National Institutes of Health grants: R01 AI063274, R01 AR056360, RC2 AR058959, P20 GM103456 (P.M.G.); R01 AR043274 (K.L.M.); N01 AR62277 (K.L.M. and J.B.H.); R37 24717, R01 AR042460, P01 AI083194, P20 RR020143, R01 DE018209 (J.B.H.); P01 AR49084 (R.P.K., J.C.E., and E.E.B.); 5UL1 RR025777 (J.C.E.), R01 AR33062 (R.P.K.); P30 AR48311 (E.E.B.); K08 AI083790, LRP AI071651, UL1 RR024999 (T.B.N.); R01 CA141700, RC1 AR058621 (M.E.A.R.); R01 AR051545-01A2, UL1 RR025014-02 (A.M.S.); P30 RR031152, U19AI082714, RC1 AR058554, P30 AR053483, N01 AI50026 (J.A.J. and J.M.G.); R21 AI070304, R01 AI070983 (S.A.B.); R01 AR43814 (B.P.T.); P60 AR053308, M01 RR-00079 (L.A.C.); R01 AR043727, UL1 RR025005 (M.A.P.), K24 AR002138, P60 2 AR30692, P01 AR49084, UL1 RR025741 (R.R.G.), 1U54 RR23417-01 (J.D.R.), R01 AR 43727, UL1RR025005 (M.A.P.), P60 AR049459 and UL1 RR029882 (D.L.K.). Additional support was obtained from the Alliance for Lupus Research (K.L.M.); Merit Award from the US Department of Veterans Affairs (J.B.H. and G.S.G.); the Swedish Research Council for Medicine, Gustaf Vth-80th Jubilee Fund and Swedish Association Against Rheumatism, Instituto de Salud Carlos III partially financed through FEDER funds of the European Community (M.E.A.R.); the European Science Foundation funds the BIOLUPUS network (M.E.A.R. coordinator); the Barrett Scholarship Fund Oklahoma Medical Research Foundation (OMRF) (C.J.L.); the Korea Healthcare Technology

Research and Development Project, Ministry for Health and Welfare, Republic of Korea (A11218-11-GM01, S.C.B.); Lupus Research Institute (T.B.N.); The Alliance for Lupus Research (T.B.N., L.A.C. and C.O.J.); the Arthritis National Research Foundation Eng Tan Scholar Award (T.B.N.); Arthritis Foundation (P.M.G. and A.M.S.); the Lupus Foundation of Minnesota (P.M.G. and K.L.M.); the Wellcome Trust (T.J.V.); Arthritis Research UK (T.J.V.); Kirkland Scholar Award (L.A.C. and J.A.J.); Wake Forest University Health Sciences Center for Public Health Genomics (C.D.L.); and the Federico Wilhelm Agricola Foundation Research grant (B.A.P.E.). The work reported on in this publication has been in part financially supported by the ESF, in the framework of the Research Networking Programme European Science Foundation - The Identification of Novel Genes and Biomarkers for Systemic Lupus Erythematosus (BIOLUPUS) 07-RNP-083.

We would like to thank Drs. Sambit Nanda and Philip Cohen (MRC Protein Phosphorylation Unit, University of Dundee, Dundee, DD1 5EH, Scotland, UK) for providing us the ABIN1 antibody as well as Dr. David W. Powell (University of Louisville School of Medicine) for his suggestions regarding the ABIN1 functional studies. We would like to express our gratitude to the SLE patients and the controls that participated in this study. We are thankful to the research assistants, coordinators and physicians that helped in the recruitment of participants. We would like to thank the following groups/individuals for contributing samples genotyped in this study: BIOLUPUS Network, GENLES Network, Dr. Peter K. Gregersen (USA), S. D'Alfonso (Italy), R. Scorza (Italy), P. Junker and H. Lastrup (Denmark), M. Bijl (Holland), E. Endreffy (Hungary), C. Vasconcelos and B.M. da Silva (Portugal), A. Suarez and C. Gutierrez (Spain), I. Rúa-Figueroa (Spain) and C. Garcilazo (Argentina). For the Asociación Andaluza de Enfermedades Autoinmunes (AADEA) collaboration: N. Ortego-Centeno (Spain), J. Jimenez-Alonso (Spain), E. de Ramon (Spain) and J. Sanchez-Roman (Spain). For the collaboration on Hispanic populations enriched for Amerindian-European admixture: M. Cardiel (Mexico), I.G. de la Torre (Mexico), M. Maradiaga (Mexico), J.F. Moctezuma (Mexico), E. Acevedo (Peru), C. Castel and M. Busajm (Argentina), and J. Musuruana (Argentina). Other participants from the Argentine Collaborative Group are: H.R. Scherbarth, P.C. Marino, E.L. Motta, S. Gamron, C. Drenkard, E. Menso, A. Allievi, G.A. Tate, J.L. Presas, S.A. Palatnik, M. Abdala, M. Bearzotti, A. Alvarellos, F. Caeiro, A. Bertoli, S. Paira, S. Roverano, C.E. Graf, E. Bertero, C. Guillerón, S. Grimaudo, J. Manni, L.J. Catoggio, E.R. Soriano, C.D. Santos, C. Prigione, F.A. Ramos, S.M. Navarro, G.A. Berbotto, M. Jorfen, E.J. Romero, M.A. Garcia, J.C. Marcos, A.I. Marcos, C.E. Perandones, A. Eimon and C.G. Battagliotti.

We thank P.S. Ramos and S. Frank for their assistance in genotyping, quality control analyses and clinical data management and the staff of the Lupus Family Registry and Repository (LFRR) for collecting and maintaining SLE samples.

References

1. Li Q, Verma IM. NF-kappaB regulation in the immune system. *Nat Rev Immunol.* 2002; 2(10):725–34. [PubMed: 12360211]
2. Wertz IE, Dixit VM. Signaling to NF-kappaB: regulation by ubiquitination. *Cold Spring Harb Perspect Biol.* 2010; 2(3):a003350. [PubMed: 20300215]
3. Heyninck K, Beyaert R. The cytokine-inducible zinc finger protein A20 inhibits IL-1-induced NF-kappaB activation at the level of TRAF6. *FEBS Lett.* 1999; 442(2–3):147–50. [PubMed: 9928991]
4. Wertz IE, O'Rourke KM, Zhou H, Eby M, Aravind L, Seshagiri S, et al. De-ubiquitination and ubiquitin ligase domains of A20 downregulate NF-kappaB signalling. *Nature.* 2004; 430(7000):694–9. [PubMed: 15258597]
5. Shembade N, Harhaj NS, Liebl DJ, Harhaj EW. Essential role for TAX1BP1 in the termination of TNF-alpha-, IL-1- and LPS-mediated NF-kappaB and JNK signaling. *EMBO J.* 2007; 26(17):3910–22. [PubMed: 17703191]
6. Heyninck K, De Valck D, Vanden Berghe W, Van Criekinge W, Contreras R, Fiers W, et al. The zinc finger protein A20 inhibits TNF-induced NF-kappaB-dependent gene expression by interfering with an RIP- or TRAF2-mediated transactivation signal and directly binds to a novel NF-kappaB-inhibiting protein ABIN. *J Cell Biol.* 1999; 145(7):1471–82. [PubMed: 10385526]
7. Ardite E, Panes J, Miranda M, Salas A, Elizalde JI, Sans M, et al. Effects of steroid treatment on activation of nuclear factor kappaB in patients with inflammatory bowel disease. *Br J Pharmacol.* 1998; 124(3):431–3. [PubMed: 9647464]
8. Feldmann M, Brennan FM, Maini RN. Role of cytokines in rheumatoid arthritis. *Annu Rev Immunol.* 1996; 14:397–440. [PubMed: 8717520]
9. Abraham E. Nuclear factor-kappaB and its role in sepsis-associated organ failure. *J Infect Dis.* 2003; 187 (Suppl 2):S364–9. [PubMed: 12792853]

10. Rayet B, Gelinas C. Aberrant rel/nfkb genes and activity in human cancer. *Oncogene*. 1999; 18(49):6938–47. [PubMed: 10602468]
11. Moser KL, Kelly JA, Lessard CJ, Harley JB. Recent insights into the genetic basis of systemic lupus erythematosus. *Genes Immun*. 2009; 10(5):373–9. [PubMed: 19440199]
12. Harley IT, Kaufman KM, Langefeld CD, Harley JB, Kelly JA. Genetic susceptibility to SLE: new insights from fine mapping and genome-wide association studies. *Nat Rev Genet*. 2009; 10(5): 285–90. [PubMed: 19337289]
13. Lessard CJ, Ice JA, Adrianto I, Wiley G, Kelly JA, Gaffney PM, et al. The genomics of autoimmune disease in the era of genome-wide association studies and beyond. *Autoimmun Rev*. 2011
14. Plenge RM, Cotsapas C, Davies L, Price AL, de Bakker PI, Maller J, et al. Two independent alleles at 6q23 associated with risk of rheumatoid arthritis. *Nat Genet*. 2007; 39(12):1477–82. [PubMed: 17982456]
15. Thomson W, Barton A, Ke X, Eyre S, Hinks A, Bowes J, et al. Rheumatoid arthritis association at 6q23. *Nat Genet*. 2007; 39(12):1431–3. [PubMed: 17982455]
16. Dieude P, Guedj M, Wipff J, Ruiz B, Riemekasten G, Matucci-Cerinic M, et al. Association of the TNFAIP3 rs5029939 variant with systemic sclerosis in the European Caucasian population. *Ann Rheum Dis*. 2010; 69(11):1958–64. [PubMed: 20511617]
17. Graham RR, Cotsapas C, Davies L, Hackett R, Lessard CJ, Leon JM, et al. Genetic variants near TNFAIP3 on 6q23 are associated with systemic lupus erythematosus. *Nat Genet*. 2008; 40(9): 1059–61. [PubMed: 19165918]
18. Musone SL, Taylor KE, Lu TT, Nititham J, Ferreira RC, Ortmann W, et al. Multiple polymorphisms in the TNFAIP3 region are independently associated with systemic lupus erythematosus. *Nat Genet*. 2008
19. Bates JS, Lessard CJ, Leon JM, Nguyen T, Battiest LJ, Rodgers J, et al. Meta-analysis and imputation identifies a 109 kb risk haplotype spanning TNFAIP3 associated with lupus nephritis and hematologic manifestations. *Genes Immun*. 2009; 10(5):470–7. [PubMed: 19387456]
20. Adrianto I, Wen F, Templeton A, Wiley G, King JB, Lessard CJ, et al. Association of a functional variant downstream of TNFAIP3 with systemic lupus erythematosus. *Nat Genet*. 2011; 43(3):253–8. [PubMed: 21336280]
21. Nair RP, Duffin KC, Helms C, Ding J, Stuart PE, Goldgar D, et al. Genome-wide scan reveals association of psoriasis with IL-23 and NF-kappaB pathways. *Nat Genet*. 2009; 41(2):199–204. [PubMed: 19169254]
22. Bowes J, Orozco G, Flynn E, Ho P, Brier R, Marzo-Ortega H, et al. Confirmation of TNIP1 and IL23A as susceptibility loci for psoriatic arthritis. *Ann Rheum Dis*. 2011; 70(9):1641–4. [PubMed: 21623003]
23. Allanore Y, Saad M, Dieude P, Avouac J, Distler JH, Amouyel P, et al. Genome-wide scan identifies TNIP1, PSORS1C1, and RHOB as novel risk loci for systemic sclerosis. *PLoS Genet*. 2011; 7(7):e1002091. [PubMed: 21750679]
24. Gateva V, Sandling JK, Hom G, Taylor KE, Chung SA, Sun X, et al. A large-scale replication study identifies TNIP1, PRDM1, JAZF1, UHRF1BP1 and IL10 as risk loci for systemic lupus erythematosus. *Nat Genet*. 2009; 41(11):1228–33. [PubMed: 19838195]
25. Han JW, Zheng HF, Cui Y, Sun LD, Ye DQ, Hu Z, et al. Genome-wide association study in a Chinese Han population identifies nine new susceptibility loci for systemic lupus erythematosus. *Nat Genet*. 2009; 41(11):1234–7. [PubMed: 19838193]
26. Hochberg MC. Updating the American College of Rheumatology revised criteria for the classification of systemic lupus erythematosus. *Arthritis Rheum*. 1997; 40(9):1725. [PubMed: 9324032]
27. Smith MW, Patterson N, Lautenberger JA, Truelove AL, McDonald GJ, Waliszewska A, et al. A high-density admixture map for disease gene discovery in african americans. *Am J Hum Genet*. 2004; 74(5):1001–13. [PubMed: 15088270]
28. Halder I, Shriver M, Thomas M, Fernandez JR, Frudakis T. A panel of ancestry informative markers for estimating individual biogeographical ancestry and admixture from four continents: utility and applications. *Hum Mutat*. 2008; 29(5):648–58. [PubMed: 18286470]

29. Price AL, Patterson NJ, Plenge RM, Weinblatt ME, Shadick NA, Reich D. Principal components analysis corrects for stratification in genome-wide association studies. *NatGenet.* 2006; 38(8):904–9.
30. Hoggart CJ, Parra EJ, Shriver MD, Bonilla C, Kittles RA, Clayton DG, et al. Control of confounding of genetic associations in stratified populations. *Am J Hum Genet.* 2003; 72(6):1492–504. [PubMed: 12817591]
31. Hoggart CJ, Shriver MD, Kittles RA, Clayton DG, McKeigue PM. Design and analysis of admixture mapping studies. *Am J Hum Genet.* 2004; 74(5):965–78. [PubMed: 15088268]
32. Purcell S, Neale B, Todd-Brown K, Thomas L, Ferreira MA, Bender D, et al. PLINK: a tool set for whole-genome association and population-based linkage analyses. *Am J Hum Genet.* 2007; 81(3):559–75. [PubMed: 17701901]
33. Pruim RJ, Welch RP, Sanna S, Teslovich TM, Chines PS, Gliedt TP, et al. LocusZoom: regional visualization of genome-wide association scan results. *Bioinformatics.* 2010; 26(18):2336–7. [PubMed: 20634204]
34. Li H, Durbin R. Fast and accurate short read alignment with Burrows-Wheeler transform. *Bioinformatics.* 2009; 25(14):1754–60. [PubMed: 19451168]
35. McKenna A, Hanna M, Banks E, Sivachenko A, Cibulskis K, Kernytzky A, et al. The Genome Analysis Toolkit: a MapReduce framework for analyzing next-generation DNA sequencing data. *Genome Res.* 2010; 20(9):1297–303. [PubMed: 20644199]
36. DePristo MA, Banks E, Poplin R, Garimella KV, Maguire JR, Hartl C, et al. A framework for variation discovery and genotyping using next-generation DNA sequencing data. *Nat Genet.* 2011; 43(5):491–8. [PubMed: 21478889]
37. Browning SR, Browning BL. Rapid and accurate haplotype phasing and missing-data inference for whole-genome association studies by use of localized haplotype clustering. *Am J Hum Genet.* 2007; 81(5):1084–97. [PubMed: 17924348]
38. Howie BN, Donnelly P, Marchini J. A flexible and accurate genotype imputation method for the next generation of genome-wide association studies. *PLoS Genet.* 2009; 5(6):e1000529. [PubMed: 19543373]
39. Danecek P, Auton A, Abecasis G, Albers CA, Banks E, DePristo MA, et al. The variant call format and VCFtools. *Bioinformatics.* 2011; 27(15):2156–8. [PubMed: 21653522]
40. Durbin RM, Abecasis GR, Altshuler DL, Auton A, Brooks LD, Gibbs RA, et al. A map of human genome variation from population-scale sequencing. *Nature.* 2010; 467(7319):1061–73. [PubMed: 20981092]
41. Marchini J, Howie B. Genotype imputation for genome-wide association studies. *Nature reviews Genetics.* 2010; 11(7):499–511.
42. Barrett JC, Fry B, Maller J, Daly MJ. Haploview: analysis and visualization of LD and haplotype maps. *Bioinformatics.* 2005; 21(2):263–5. [PubMed: 15297300]
43. Rasmussen A, Sevier S, Kelly JA, Glenn SB, Aberle T, Cooney CM, et al. The lupus family registry and repository. *Rheumatology (Oxford).* 2011; 50(1):47–59. [PubMed: 20864496]
44. Nanda SK, Venigalla RK, Ordureau A, Patterson-Kane JC, Powell DW, Toth R, et al. Polyubiquitin binding to ABIN1 is required to prevent autoimmunity. *J Exp Med.* 2011; 208(6):1215–28. [PubMed: 21606507]
45. Wagner S, Carpentier I, Rogov V, Kreike M, Ikeda F, Lohr F, et al. Ubiquitin binding mediates the NF-kappaB inhibitory potential of ABIN proteins. *Oncogene.* 2008; 27(26):3739–45. [PubMed: 18212736]
46. Oshima S, Turer EE, Callahan JA, Chai S, Advincula R, Barrera J, et al. ABIN-1 is a ubiquitin sensor that restricts cell death and sustains embryonic development. *Nature.* 2009; 457(7231):906–9. [PubMed: 19060883]
47. Zhou J, Wu R, High AA, Slaughter CA, Finkelstein D, Rehg JE, et al. A20-binding inhibitor of NF-kappaB (ABIN1) controls Toll-like receptor-mediated CCAAT/enhancer-binding protein beta activation and protects from inflammatory disease. *Proceedings of the National Academy of Sciences of the United States of America.* 2011; 108(44):E998–1006. [PubMed: 22011580]

48. Adzhubei IA, Schmidt S, Peshkin L, Ramensky VE, Gerasimova A, Bork P, et al. A method and server for predicting damaging missense mutations. *Nat Methods*. 2010; 7(4):248–9. [PubMed: 20354512]
49. Gurevich I, Zhang C, Encarnacao PC, Struzynski CP, Livings SE, Aneskievich BJ. PPARgamma and NF-kappaB regulate the gene promoter activity of their shared repressor, TNIP1. *Biochimica et biophysica acta*. 2012; 1819(1):1–15. [PubMed: 22001530]
50. Nath SK, Han S, Kim-Howard X, Kelly JA, Viswanathan P, Gilkeson GS, et al. A nonsynonymous functional variant in integrin-alpha(M) (encoded by ITGAM) is associated with systemic lupus erythematosus. *Nat Genet*. 2008; 40(2):152–4. [PubMed: 18204448]

\$watermark-text

\$watermark-text

\$watermark-text

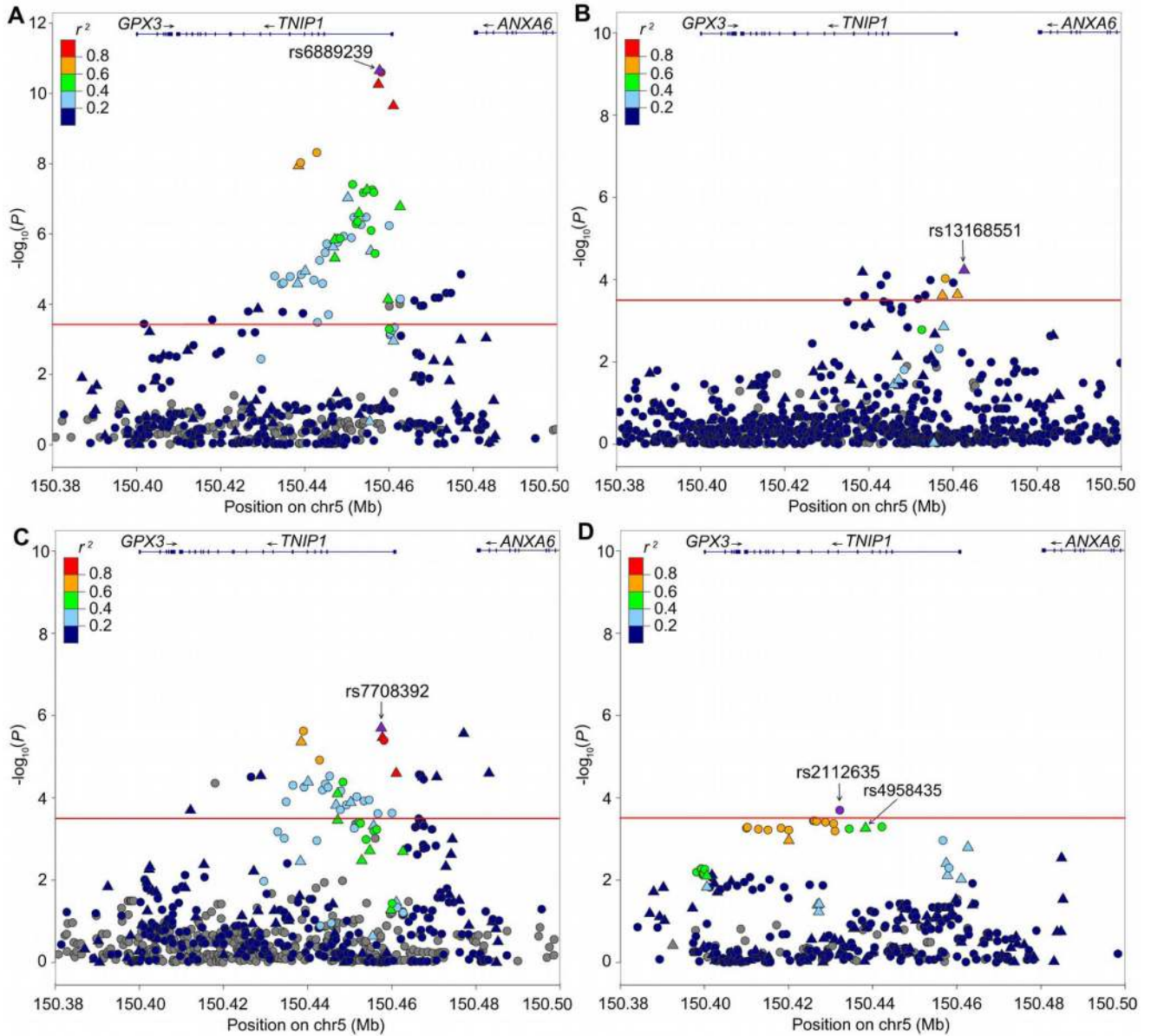


Figure 1. SNPs in and around the *TNIP1* region associated with SLE in (A) European-ancestry (B) African-American, (C) Hispanic, and (D) East Asian populations. Genotyped SNPs are represented by triangles and imputed SNPs are shown in circles. The red solid line refers to the Bonferroni threshold of significance. The color of each triangle or circles represents the level of linkage disequilibrium (LD) between each SNP and the most significant SNP.

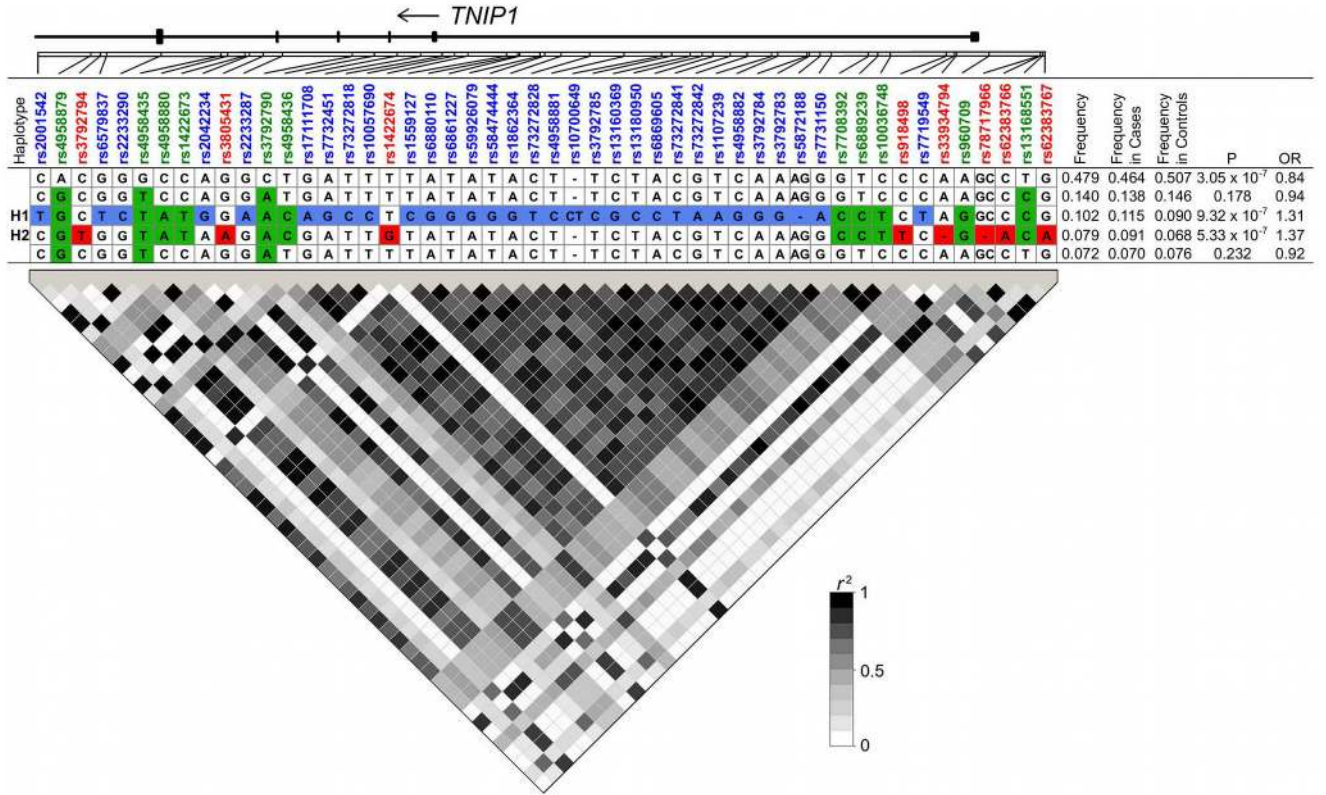


Figure 2. *TNIP1* haplotypes and linkage disequilibrium (LD) for SLE-associated variants that surpassed the Bonferroni correction threshold of $P < 3.21 \times 10^{-4}$ in European-ancestry population. Haplotypes are shown at a frequency > 3%. The group of variants unique to H1, H2, or shared by H1 and H2 haplotypes, are colored in blue, red, and green, respectively. In the haplotype block, white boxes represent the major alleles and colored boxes represent the minor alleles (colored according to their group). Pairwise LD relationships (r^2) are shown below the haplotype block with different color intensities according to degree of correlation between two variants.

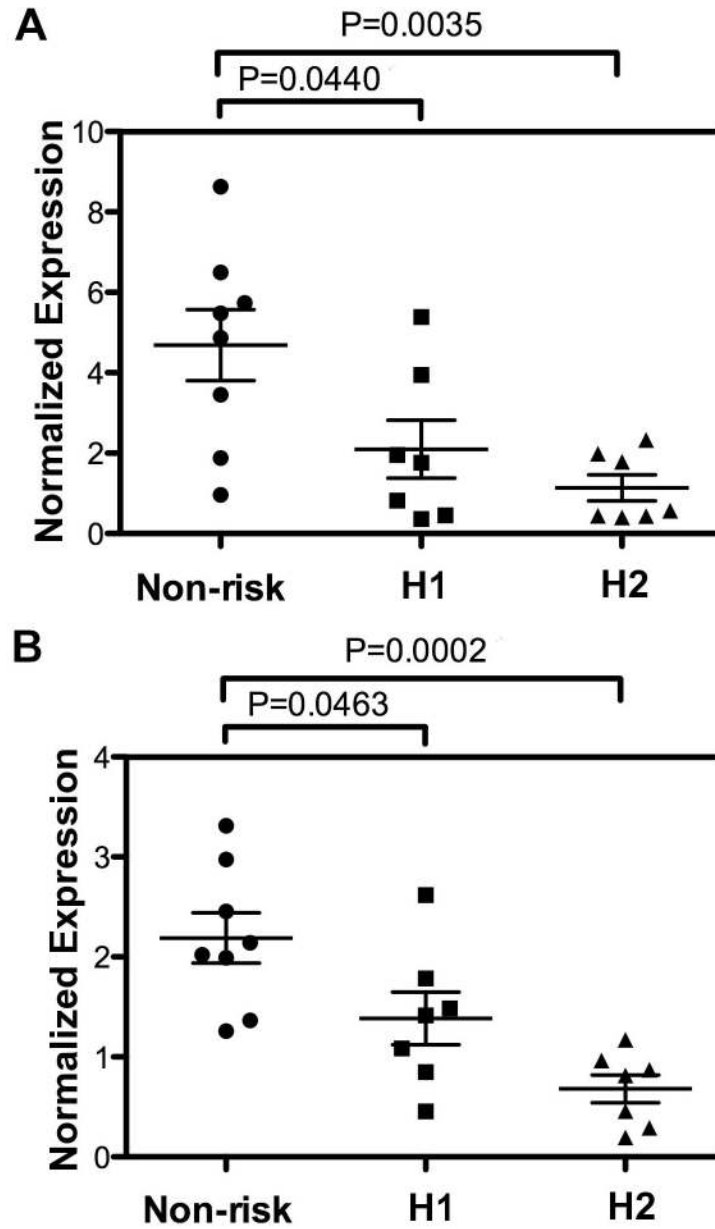


Figure 3. Effect of the risk haplotypes on (A) *TNIP1* mRNA and (B) ABIN1 protein expression. On the X-axis, the three different haplotypes are displayed corresponding to the non-risk, H1, and H2 haplotypes. On the Y-axis is the level of normalized expression for each assay. Each data point represents the expression level of *TNIP1* mRNA or ABIN1 protein for one individual. Significant differences from the mean expression of the non-risk haplotype were determined using an unpaired *t*-test.

Table 1

Sample summary following quality control adjustments.

Population	Number of Samples	Case	Control	Male	Female
European-ancestry	7427	3936	3491	1495	5932
African American	3338	1527	1811	695	2643
Hispanic*	2299	1492	807	207	2092
East Asian	2525	1265	1260	253	2272
African American-Gullah	275	152	123	33	242
Total	15864	8372	7492	2683	13181

* Enriched for Amerindian-European admixture.

Table 2
 Association evidence for variants within *TNIP1* with $P < 3.21 \times 10^{-4}$ in European-ancestry population.

SNP	bp (hg19)	Variant Status^a	Imputation Info Score	Alleles^b	MAF^c	OR(95% CI)^d	P^e
rs2001542	150432859	i-ITGP	0.880	C/T	0.111	1.28(1.16–1.42)	1.57E-05
rs4958879	150434422	i-ITGP	0.936	A/G	0.482	1.19(1.11–1.26)	2.64E-05
rs3792794	150434722	i-ITGP	0.961	C/T	0.084	1.32(1.17–1.49)	1.66E-04
rs6579837	150434894	i-ITGP	0.929	G/T	0.116	1.28(1.16–1.42)	2.45E-05
rs2233290	150436503	i-ITGP	0.984	G/C	0.110	1.31(1.18–1.45)	1.63E-05
rs4958435	150438284	g	1.000	G/T	0.487	1.16(1.08–1.24)	2.60E-05
rs4958880	150438477	g	1.000	C/A	0.225	1.27(1.17–1.38)	1.15E-08
rs14222673	150438988	i-ITGP	0.991	C/T	0.225	1.32(1.22–1.42)	9.35E-09
rs2042234	150439131	i-ITGP	0.990	A/G	0.110	1.31(1.18–1.45)	1.43E-05
rs3805431	150439539	i-ITGP	0.973	G/A	0.084	1.32(1.17–1.48)	1.82E-04
rs2233287	150440097	g	1.000	G/A	0.110	1.28(1.14–1.42)	1.15E-05
rs3792790	150442171	i-ITGP	0.970	C/A	0.486	1.18(1.11–1.26)	2.06E-05
rs4958436	150442829	i-ITGP	0.976	T/C	0.237	1.32(1.22–1.42)	4.81E-09
rs17111708	150443507	i-ITGP	0.982	G/A	0.111	1.32(1.19–1.47)	5.65E-06
rs7732451	150444212	i-ITGP	0.982	A/G	0.141	1.26(1.15–1.38)	2.57E-05
rs73272818	150444843	i-ITGP	0.986	T/C	0.110	1.33(1.2–1.48)	3.40E-06
rs10057690	150445215	i-ITGP	0.984	T/C	0.112	1.34(1.21–1.49)	1.91E-06
rs1422674	150445609	i-ITGP	0.960	T/G	0.101	1.3(1.17–1.45)	1.98E-04
rs1559127	150446753	g	1.000	T/C	0.131	1.28(1.16–1.42)	2.55E-06
rs6880110	150447090	g	1.000	A/G	0.169	1.25(1.14–1.37)	1.47E-06
rs6861227	150447128	g	1.000	T/G	0.168	1.24(1.13–1.36)	4.88E-06
rs59926079	150447743	i-ITGP	0.982	A/G	0.112	1.34(1.21–1.49)	1.32E-06
rs58474444	150447880	i-ITGP	0.988	T/G	0.110	1.34(1.2–1.48)	1.70E-06
rs1862364	150448376	i-ITGP	0.987	A/G	0.170	1.27(1.16–1.38)	1.33E-06
rs73272828	150449220	i-ITGP	0.985	C/T	0.112	1.35(1.21–1.49)	1.17E-06
rs4958881	150450236	g	1.000	T/C	0.140	1.31(1.19–1.45)	9.34E-08
rs10700649	150451347	i-seq	0.984	C/CCCT	0.152	1.32(1.2–1.45)	3.90E-08
rs3792785	150451650	i-ITGP	0.983	T/C	0.123	1.34(1.21–1.48)	3.37E-07

SNP	bp (hg19)	Variant Status ^a	Imputation Info Score	Alleles ^b	MAF ^c	OR(95% CI) ^d	P ^e
rs13160369	150452196	i-ITGP	0.985	C/G	0.180	1.27(1.16–1.38)	5.16E-07
rs13180950	150452553	i-ITGP	0.986	T/C	0.182	1.27(1.16–1.38)	4.39E-07
rs6869605	150452866	g	1.000	A/C	0.147	1.29(1.17–1.43)	2.56E-07
rs73272841	150453384	i-ITGP	0.978	C/T	0.123	1.33(1.2–1.47)	5.42E-07
rs73272842	150453888	i-ITGP	0.983	G/A	0.149	1.31(1.2–1.44)	6.66E-08
rs1107239	150454606	i-ITGP	0.985	T/A	0.123	1.33(1.21–1.47)	3.35E-07
rs4958882	150454787	g	1.000	C/G	0.149	1.31(1.19–1.44)	5.64E-08
rs3792784	150455672	g	1.000	A/G	0.119	1.29(1.16–1.43)	3.06E-06
rs3792783	150455732	i-ITGP	0.988	A/G	0.178	1.26(1.16–1.37)	7.94E-07
rs5872188	150456053	i-seq	0.988	CAG/C	0.150	1.32(1.2–1.43)	5.51E-08
rs7731150	150456392	i-ITGP	0.986	G/A	0.150	1.31(1.2–1.44)	6.53E-08
rs7708392	150457485	g	0.989	G/C	0.284	1.29(1.2–1.39)	5.51E-11
rs6889239	150457771	g	1.000	T/C	0.285	1.3(1.2–1.4)	2.24E-11
rs10036748	150458146	i-ITGP	0.988	C/T	0.283	1.33(1.24–1.43)	2.50E-11
rs918498	150459788	g	1.000	C/T	0.129	1.23(1.11–1.37)	7.29E-05
rs7719549	150460047	i-ITGP	0.965	C/T	0.126	1.32(1.2–1.46)	5.81E-07
rs3934794	150460088	i-seq	0.984	GA/G	0.129	1.27(1.15–1.39)	1.14E-04
rs960709	150461049	g	1.000	A/G	0.282	1.28(1.19–1.39)	2.25E-10
rs78717966	150462573	i-seq	0.932	GGC/G	0.094	1.33(1.19–1.49)	7.67E-05
rs62383766	150462576	i-seq	0.913	C/A	0.092	1.32(1.18–1.48)	9.75E-05
rs13168551	150462638	g	1.000	T/C	0.441	1.2(1.12–1.29)	1.66E-07
rs62383767	150462705	i-ITGP	0.924	G/A	0.095	1.32(1.18–1.48)	7.10E-05

^aVariant Status: genotyped (g), imputed from the 1000 Genomes Project data (i-ITGP), or imputed from sequencing data (i-seq).

^bMajor/minor.

^cMinor allele frequency.

^dThe odds ratio (OR) was calculated with respect to the minor allele.

^eAdjusted for gender and global ancestry estimates.

\$watermark-text

\$watermark-text

\$watermark-text

Table 3

Summary of haplotype analyses in European-ancestry, African-American, Hispanic, and East Asian populations. Two independent risk haplotypes were observed in European-ancestry, African-American, and Hispanic populations. However, only the H2 risk haplotype was found in East Asians.

Population	H1 Risk Haplotype				H2 Risk Haplotype					
	Freq.	Freq. in Cases	Freq. in Controls	P	OR	Freq.	Freq. in Cases	Freq. in Controls	P	OR
European-ancestry (Figure 2)	0.102	0.115	0.090	9.32×10^{-7}	1.31	0.079	0.091	0.068	5.33×10^{-7}	1.37
African American (Supplementary Figure 6A)	0.133	0.153	0.121	3.00×10^{-4}	1.31	0.020	0.024	0.017	0.047	1.42
Hispanic (Supplementary Figure 6B)	0.090	0.101	0.072	0.002	1.45	0.285	0.314	0.245	1.66×10^{-6}	1.41
East Asian (Supplementary Figure 6C)	N/A	N/A	N/A	N/A	N/A	0.531	0.542	0.527	0.295	1.06

* N/A, not available.